

4 DISTRIBUTED ARRAYS IN A NON-MULTIPATH ENVIRONMENT

4.1 Introduction

In this chapter the performance of distributed arrays is investigated in a non-multipath environment. Firstly, an analytical expression is derived for the output signal to interference plus noise ratio (SINR) of two distributed arrays with independent beamforming of each array as well as for optimum combining of the two array output signals. A single stationary desired mobile in the presence of stationary interferer is considered. It is then shown that the SINR obtained with optimum combining of the two array output signals is equal to the sum of the SINRs of the individual arrays. Following this, it will be shown analytically that the SINR of the two distributed arrays with combined beamforming is always greater than the SINR with independent beamforming. It will then be demonstrated with simulation results that the analytical results can be extended to multiple interferers. This is followed by simulation results of the signal to noise ratios for distributed arrays with and without power control. The simulations are first done for one of the distributed arrays, followed by all three distributed arrays with mobiles located in a single cell. A seven cell network is then simulated with a reuse factor of three.

4.2 Analytical Investigation of the SINR Performance of Distributed Arrays

4.2.1 SINR of Independent Beamforming of Each Array

Consider two arrays, each with optimum beamforming for the desired signal. It will be shown analytically in this section that the SINR with optimum combining of the output signals of two distributed arrays is the sum of the SINRs of the individual arrays. The geometry under consideration is shown in Figure 30. The system consists of two arrays at the corners of the cell, each having two elements. A desired signal is located at the center of the cell and one interferer is located at an angle of ψ relative to the boresight of arrays 1 and 2. The array elements are spaced a half wavelength apart and fading, pathloss and propagation delays between sub-arrays are ignored for this analysis³⁵.

³⁵ The effect of fading and pathloss will be included in later chapters using numerical methods.

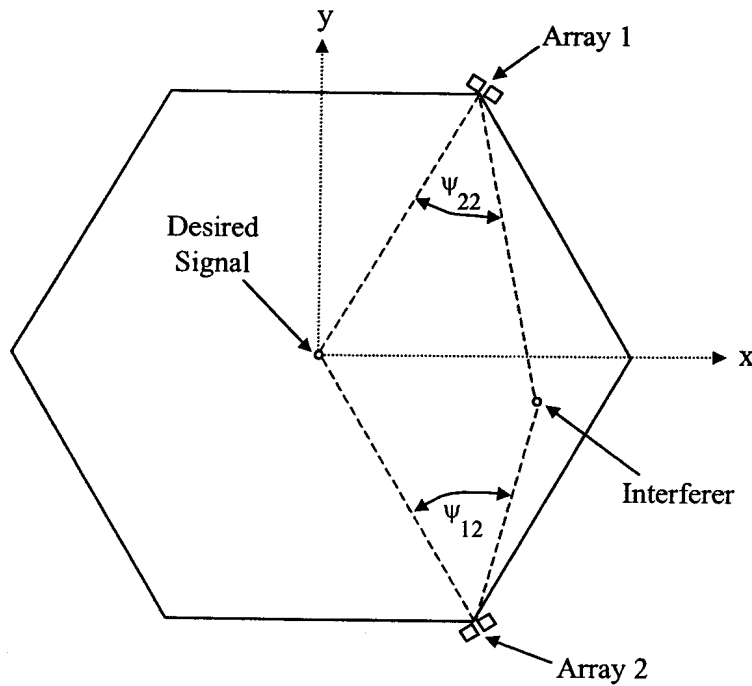


Figure 30: Geometry of two distributed arrays with one interferer.

The received signals at each individual array is combined with optimum beamforming, followed by optimum combining of the two array output signals, as shown in Figure 31.

The output of the individual arrays is:

$$\mathbf{Y}_1 = \mathbf{W}_1^H \mathbf{X}_1 = [W_{11}^* \ W_{12}^*] \begin{bmatrix} X_{11} \\ X_{12} \end{bmatrix} \quad (85)$$

and

$$\mathbf{Y}_2 = \mathbf{W}_2^H \mathbf{X}_2 = [W_{21}^* \ W_{22}^*] \begin{bmatrix} X_{21} \\ X_{22} \end{bmatrix} \quad (86)$$

where \mathbf{W}_1 is the weight vector and \mathbf{X}_1 is the received signal vector of array 1 and \mathbf{W}_2 is the weight vector and \mathbf{X}_2 is the received signal vector of array 2.

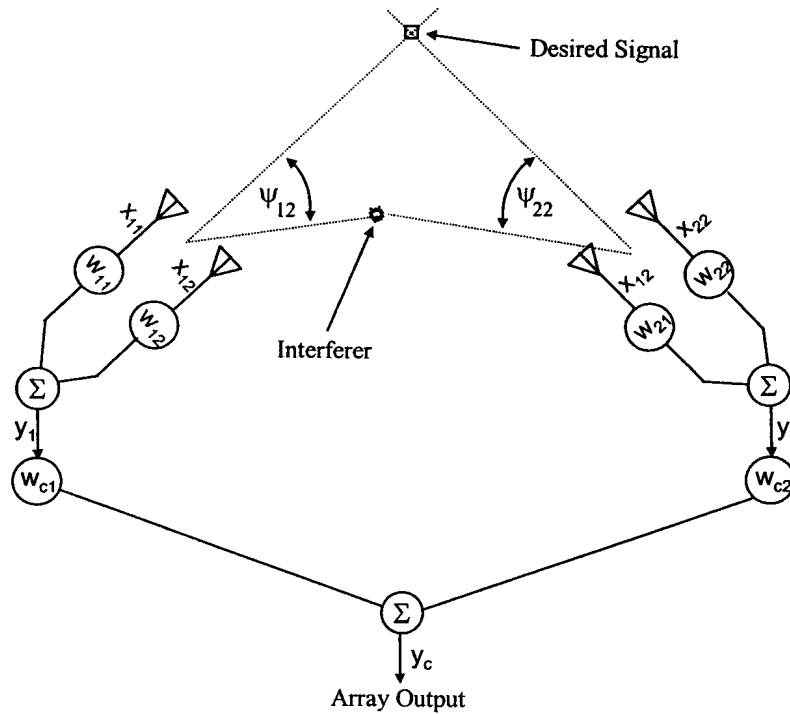


Figure 31: Independent array beamforming geometry.

Optimum combining of the output signals of the two array outputs gives the total array output signal:

$$y_c = \mathbf{W}_c^H \begin{bmatrix} \mathbf{W}_1^H \mathbf{X}_1 \\ \mathbf{W}_2^H \mathbf{X}_2 \end{bmatrix} \quad (87)$$

where \mathbf{W}_c is the total array weight vector (see Figure 32). The weight vector \mathbf{W}_c for optimum combining of the arrays is [54]:

$$\mathbf{W}_c = \mu_{wc} \mathbf{R}_{nnC}^{-1} \mathbf{U}_d \quad (88)$$

where \mathbf{R}_{nnC} is the total array interference plus noise covariance matrix of the combined array, μ_{wc} is a constant that constrains the array to have a unity response in the direction of the desired signal³⁶ and \mathbf{U}_d is the desired signal propagation vector, given as:

$$\mathbf{U}_d = [1 \ 1]^T \quad (89)$$

The constraint μ_{wc} is [54]:

³⁶ Referred to as the look direction in [54].

$$\mu_{wc} = \frac{1}{\mathbf{U}_d^H \mathbf{R}_{nnC}^{-1} \mathbf{U}_d} \quad (90)$$

The covariance matrix \mathbf{R}_{nnC} is:

$$\mathbf{R}_{nnC} = E \left\{ \begin{bmatrix} \mathbf{W}_1^H \mathbf{X}_{Q1} \\ \mathbf{W}_2^H \mathbf{X}_{Q2} \end{bmatrix} \begin{bmatrix} \mathbf{W}_1^H \mathbf{X}_{Q1} & \mathbf{W}_2^H \mathbf{X}_{Q2} \end{bmatrix}^H \right\} \quad (91)$$

with \mathbf{X}_{Q1} and \mathbf{X}_{Q2} is array 1 and 2 interferer plus noise receive vectors. Multiplying the factors in equation (91), the following is obtained:

$$\mathbf{R}_{nnC} = \begin{bmatrix} \mathbf{W}_1^H E(\mathbf{X}_{Q1} \mathbf{X}_{Q1}^H) \mathbf{W}_1 & \mathbf{W}_1^H E(\mathbf{X}_{Q1} \mathbf{X}_{Q2}^H) \mathbf{W}_2 \\ \mathbf{W}_2^H E(\mathbf{X}_{Q2} \mathbf{X}_{Q1}^H) \mathbf{W}_1 & \mathbf{W}_2^H E(\mathbf{X}_{Q2} \mathbf{X}_{Q2}^H) \mathbf{W}_2 \end{bmatrix} \quad (92)$$

which can be re-written as:

$$\mathbf{R}_{nnC} = \begin{bmatrix} \mathbf{W}_1^H \mathbf{R}_{nn,11} \mathbf{W}_1 & \mathbf{W}_1^H \mathbf{R}_{nn,12} \mathbf{W}_2 \\ \mathbf{W}_2^H \mathbf{R}_{nn,21} \mathbf{W}_1 & \mathbf{W}_2^H \mathbf{R}_{nn,22} \mathbf{W}_2 \end{bmatrix} = \begin{bmatrix} \mathbf{R}_{nnC,11} & \mathbf{R}_{nnC,12} \\ \mathbf{R}_{nnC,21} & \mathbf{R}_{nnC,22} \end{bmatrix} \quad (93)$$

with $\mathbf{R}_{nn,11}$, $\mathbf{R}_{nn,12}$, $\mathbf{R}_{nn,21}$ and $\mathbf{R}_{nn,22}$ the covariance matrices of the received interference plus noise signals of array 1 and 2. Assuming now that the power levels of the desired and interfering signals are equal to one, the propagation environment is lossless and $\psi_{22} = \psi_{12}$, the signals arriving at the two arrays are:

$$\mathbf{X}_{Q1} = S_Q \mathbf{U}_{Q1} + \mathbf{n}_1 = S_Q \begin{bmatrix} e^{j(\pi/2) \sin \psi_{12}} & e^{-j(\pi/2) \sin \psi_{12}} \end{bmatrix}^T + [\mathbf{n}_{11} \ \mathbf{n}_{12}]^T \quad (94)$$

and

$$\mathbf{X}_{Q2} = S_Q \mathbf{U}_{Q2} + \mathbf{n}_2 = S_Q \begin{bmatrix} e^{-j(\pi/2) \sin \psi_{22}} & e^{j(\pi/2) \sin \psi_{22}} \end{bmatrix}^T + [\mathbf{n}_{21} \ \mathbf{n}_{22}]^T \quad (95)$$

where S_Q is the amplitude of the interference signal bits, \mathbf{n} is the array element noise vector and \mathbf{U}_Q is the interference signal array vector. It is assumed that the noise is Gaussian and uncorrelated between the array elements. Using (92), the component (1,1) of covariance matrices in (93) becomes:

$$\mathbf{R}_{nn,11} = E \left\{ \begin{bmatrix} S_Q e^{j(\pi/2)\sin \psi_{12}} + \mathbf{n}_{11} \\ S_Q e^{-j(\pi/2)\sin \psi_{12}} + \mathbf{n}_{12} \end{bmatrix} \begin{bmatrix} S_Q^* e^{-j(\pi/2)\sin \psi_{12}} + \mathbf{n}_{11}^* & -S_Q^* e^{j(\pi/2)\sin \psi_{12}} + \mathbf{n}_{12}^* \end{bmatrix} \right\} \quad (96)$$

$$= \begin{bmatrix} R_{nn,11}(1,1) & R_{nn,11}(1,2) \\ R_{nn,11}(2,1) & R_{nn,11}(2,2) \end{bmatrix} \quad (97)$$

where:

$$R_{nn,11}(1,1) = E(S_Q S_Q^*) + E(S_Q e^{j(\pi/2)\sin \psi_{12}} \mathbf{n}_{11}^*) + E(\mathbf{n}_{11} S_Q^* e^{-j(\pi/2)\sin \psi_{12}}) + E(\mathbf{n}_{11} \mathbf{n}_{11}^*) \quad (98)$$

$$\begin{aligned} R_{nn,11}(1,2) &= E(S_Q S_Q^*) e^{j\pi \sin \psi_{12}} + E(S_Q e^{j(\pi/2)\sin \psi_{12}} \mathbf{n}_{12}^*) \\ &+ E(\mathbf{n}_{11} S_Q^* e^{j(\pi/2)\sin \psi_{12}}) + E(\mathbf{n}_{11} \mathbf{n}_{12}^*) \end{aligned} \quad (99)$$

$$\begin{aligned} R_{nn,11}(2,1) &= E(S_Q S_Q^*) e^{-j\pi \sin \psi_{22}} + E(S_Q e^{-j(\pi/2)\sin \psi_{22}} \mathbf{n}_{11}^*) \\ &+ E(\mathbf{n}_{12} S_Q^* e^{-j(\pi/2)\sin \psi_{12}}) + E(\mathbf{n}_{12} \mathbf{n}_{11}^*) \end{aligned} \quad (100)$$

$$R_{nn,11}(2,2) = E(S_Q S_Q^*) + E(S_Q e^{-j(\pi/2)\sin \psi_{12}} \mathbf{n}_{12}^*) + E(\mathbf{n}_{12} S_Q^* e^{j(\pi/2)\sin \psi_{12}}) + E(\mathbf{n}_{12} \mathbf{n}_{12}^*) \quad (101)$$

Using the fact that the signals are uncorrelated with each other as well as with the noise, the matrix $\mathbf{R}_{nn,11}$ becomes:

$$\mathbf{R}_{nn,11} = \begin{bmatrix} 1 + \sigma^2 & e^{j\pi \sin \psi_{12}} \\ e^{-j\pi \sin \psi_{12}} & 1 + \sigma^2 \end{bmatrix} \quad (102)$$

Similarly, the co-variance matrices $\mathbf{R}_{nn,12}$ $\mathbf{R}_{nn,21}$ $\mathbf{R}_{nn,22}$ are:

$$\mathbf{R}_{nn,12} = \begin{bmatrix} e^{j(\pi/2)(\sin \psi_{12} + \sin \psi_{22})} & e^{j(\pi/2)(\sin \psi_{12} - \sin \psi_{22})} \\ e^{-j(\pi/2)(\sin \psi_{12} - \sin \psi_{22})} & e^{-j(\pi/2)(\sin \psi_{12} + \sin \psi_{22})} \end{bmatrix} \quad (103)$$

$$\mathbf{R}_{nn,21} = \begin{bmatrix} e^{-j(\pi/2)(\sin \psi_{22} + \sin \psi_{12})} & e^{-j(\pi/2)(\sin \psi_{22} - \sin \psi_{12})} \\ e^{j(\pi/2)(\sin \psi_{22} - \sin \psi_{12})} & e^{j(\pi/2)(\sin \psi_{22} + \sin \psi_{12})} \end{bmatrix} \quad (104)$$

and

$$\mathbf{R}_{nn,22} = \begin{bmatrix} 1 + \sigma^2 & e^{-j\pi \sin \psi_{12}} \\ e^{j\pi \sin \psi_{12}} & 1 + \sigma^2 \end{bmatrix} \quad (105)$$

From (88) and (102), the independent array optimum combining weight vectors after some manipulation become:

$$\mathbf{W}_1 = \mu_{wcl} \mathbf{R}_{nn,11}^{-1} \mathbf{U}_d = \begin{bmatrix} \frac{0.5(e^{j\pi \sin \psi_{12}} - \sigma^4 - 1)}{\cos(\pi \sin \psi_{12}) - \sigma^4 - 1} \\ \frac{0.5(e^{-j\pi \sin \psi_{12}} - \sigma^4 - 1)}{\cos(\pi \sin \psi_{12}) - \sigma^4 - 1} \end{bmatrix} \quad (106)$$

and

$$\mathbf{W}_2 = \mu_{wcl} \mathbf{R}_{Q,22}^{-1} \mathbf{U}_d = \begin{bmatrix} \frac{0.5(e^{-j\pi \sin \psi_{22}} - \sigma^4 - 1)}{\cos(\pi \sin \psi_{22}) - \sigma^4 - 1} \\ \frac{0.5(e^{j\pi \sin \psi_{22}} - \sigma^4 - 1)}{\cos(\pi \sin \psi_{22}) - \sigma^4 - 1} \end{bmatrix} \quad (107)$$

The SINR of array 1 is given by [54]:

$$\text{SINR}_1 = \mathbf{U}_d^H \mathbf{R}_{Q,11}^{-1} \mathbf{U}_d = 2 \frac{\sigma^2 + 1 - \cos(\pi \sin \psi_{12})}{(\sigma^2 + 2)\sigma^2} \quad (108)$$

and array 2:

$$\text{SINR}_2 = \mathbf{U}_d^H \mathbf{R}_{Q,22}^{-1} \mathbf{U}_d = 2 \frac{\sigma^2 + 1 - \cos(\pi \sin \psi_{22})}{(\sigma^2 + 2)\sigma^2} \quad (109)$$

Since $\sigma^2 \ll 1$ and for the case where $\psi_{12} \neq 0$, the SINR of array1 reduces to:

$$\text{SINR}_1 = 2 \frac{1 - \cos(\pi \sin \psi_{12})}{\sigma^2} \quad (110)$$

and array 2:

$$\text{SINR}_2 = 2 \frac{1 - \cos(\pi \sin \psi_{22})}{\sigma^2} \quad (111)$$

The cumulative SINR of both arrays is:

$$\text{SINR}_1 + \text{SINR}_2 = 2 \left(\frac{2 - \cos(\pi \sin \psi_{12}) - \cos(\pi \sin \psi_{22})}{\sigma^2} \right) \quad (112)$$

Consider now a simplified case where $\psi_{22} = \psi_{12}$ ³⁷. In this case the SINR of array 1 and array 2 are equal, with the total SINR of (112) simplifying to:

$$\text{SINR}_1 + \text{SINR}_2 = 2 \frac{1 - \cos(\pi \sin \psi_{12})}{\sigma^2} \quad (113)$$

The combined covariance matrix in (93) in the case where $\psi_{22} = \psi_{12}$ reduces to:

$$\mathbf{R}_{\text{nnC},11} = \mathbf{R}_{\text{nnC},22} = \frac{-0.5\sigma^4(\sigma^4 + 2)}{\cos(\pi \sin \psi_{12}) - \sigma^4 - 1} \quad (114)$$

and

$$\mathbf{R}_{\text{nnC},12} = \mathbf{R}_{\text{nnC},21} = \frac{0.5(\sigma^4[\cos(\pi \sin \psi_{12}) + 1])}{\cos^2(\pi \sin \psi_{12}) - 2\cos(\pi \sin \psi_{12}) - \sigma^4 \cos(\pi \sin \psi_{12}) + (\sigma^4 + 1)^2} \quad (115)$$

The SINR of the arrays combined with optimum combining is [54]:

$$\text{SINR}_C = \mathbf{U}_{\text{dc}}^H \mathbf{R}_{\text{nnC}}^{-1} \mathbf{U}_{\text{dc}} \quad (116)$$

where \mathbf{U}_{dc} is the desired signal propagation or steering vector for the combined array, given by:

$$\mathbf{U}_{\text{dc}} = [1 \ 1]^T \quad (117)$$

Using (93), (114), (115) and (116) and with simplification, the SINR becomes:

$$\text{SINR}_C = 4 \frac{(\sigma^2 + 1)^2 + \cos^2(\pi \sin \psi_{12}) - 2\cos(\pi \sin \psi_{12}) - 2\sigma^2 \cos(\pi \sin \psi_{12})}{(\sigma^4 + 4\sigma^2 - 2\cos(\pi \sin \psi_{12}) + 2)\sigma^2} \quad (118)$$

which reduce to the following when $\sigma^2 \ll 1$:

$$\text{SINR}_C = 2 \frac{1 - \cos(\pi \sin \psi_{12})}{\sigma^2} \quad (119)$$

which is equal to the SINR of the individual arrays in (113). It is shown in Appendix B that the result is valid for the more general case where $\psi_{22} \neq \psi_{12}$.

³⁷ The general case where $\psi_{22} \neq \psi_{12}$ is given in Appendix B.

4.2.2 SINR of Arrays with Combined Beamforming

Consider the combined beamforming of both arrays as depicted Figure 32. The propagation delays between the sub-arrays are not included here. The desired signal received at the combined array elements is:

$$\mathbf{U}_d = [1 \ 1 \ 1 \ 1]^T \quad (120)$$

and the interference plus noise received at the array elements are:

$$\mathbf{X}_Q = \mathbf{S}_Q \mathbf{U}_Q + \mathbf{n} = \mathbf{S}_Q \begin{bmatrix} e^{j\pi \sin \psi_{12}} & e^{-j\pi \sin \psi_{12}} & e^{-j\pi \sin \psi_{22}} & e^{j\pi \sin \psi_{22}} \end{bmatrix}^T + \mathbf{n} \quad (121)$$

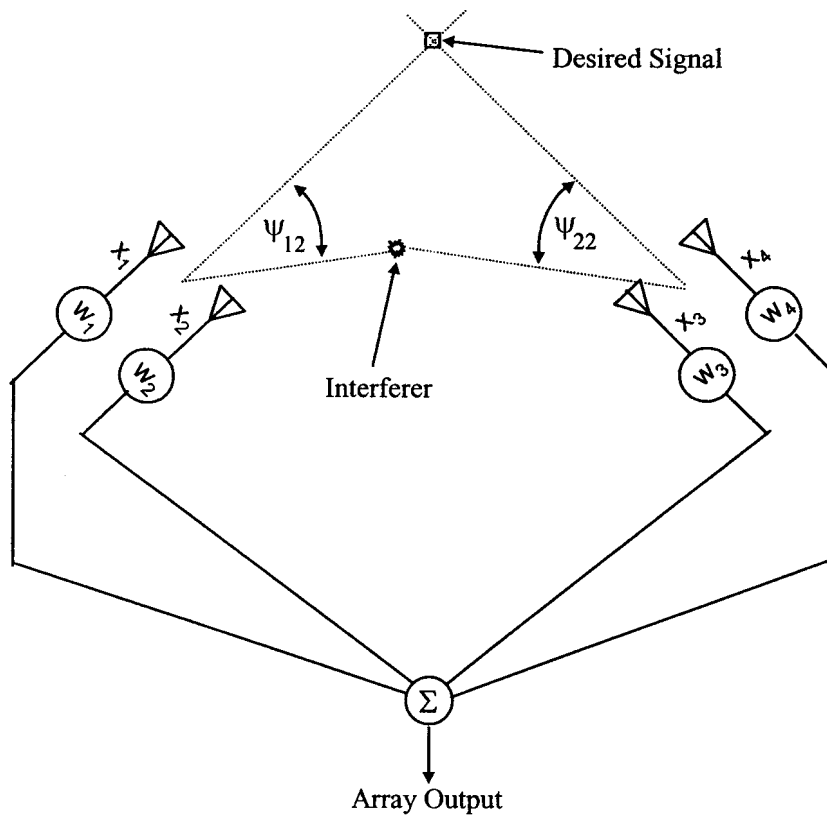


Figure 32: Combined array beamforming geometry.

The received interference plus noise co-variance matrix is [54]:

$$\mathbf{R}_{nn} = E \{ \mathbf{X}_Q \mathbf{X}_Q^H \} \quad (122)$$

Using (121) in (122), the received interference plus noise co-variance matrix is:

$$\mathbf{R}_{nn} = E \left\{ \mathbf{S}_Q \mathbf{S}_Q^* \right\} \begin{bmatrix} e^{j\pi \sin \psi_{12}} \\ e^{-j\pi \sin \psi_{12}} \\ e^{-j\pi \sin \psi_{22}} \\ e^{j\pi \sin \psi_{22}} \end{bmatrix} \begin{bmatrix} e^{-j\pi \sin \psi_{22}} & e^{j\pi \sin \psi_{22}} & e^{j\pi \sin \psi_{22}} & e^{-j\pi \sin \psi_{22}} \end{bmatrix} + \sigma^2 \mathbf{I} \quad (123)$$

Since $E \left\{ \mathbf{S}_Q \mathbf{S}_Q^* \right\}$ is unity, the co-variance matrix in (122) becomes:

$$\mathbf{R}_{nn} = \begin{bmatrix} 1 + \sigma^2 & e^{j\pi \sin \psi_{12}} & e^{j(\pi/2)(\sin \psi_{12} + \sin \psi_{22})} & e^{j(\pi/2)(\sin \psi_{12} - \sin \psi_{22})} \\ e^{-j\pi \sin \psi_{12}} & 1 + \sigma^2 & e^{-j(\pi/2)(\sin \psi_{12} - \sin \psi_{22})} & e^{-j(\pi/2)(\sin \psi_{12} + \sin \psi_{22})} \\ e^{-j(\pi/2)(\sin \psi_{12} + \sin \psi_{22})} & e^{-j(\pi/2)(\sin \psi_{22} - \sin \psi_{21})} & 1 + \sigma^2 & e^{-j\pi \sin \psi_{22}} \\ e^{j(\pi/2)(\sin \psi_{22} - \sin \psi_{12})} & e^{j(\pi/2)(\sin \psi_{12} + \sin \psi_{22})} & e^{j\pi \sin \psi_{22}} & 1 + \sigma^2 \end{bmatrix} \quad (124)$$

The inverse of the co-variance matrix \mathbf{R}_{nn} is:

$$\mathbf{R}_{nn}^{-1} = \frac{1}{c} \begin{bmatrix} \sigma^2 + 3 & -e^{j\pi \sin \psi_{12}} & -e^{j(\pi/2)\alpha_1} & -e^{j(\pi/2)\alpha_2} \\ -e^{-j\pi \sin \psi_{12}} & \sigma^2 + 3 & -e^{-j(\pi/2)\alpha_2} & -e^{j(\pi/2)\alpha_1} \\ -e^{-j(\pi/2)\alpha_1} & -e^{j(\pi/2)\alpha_2} & \sigma^2 + 3 & -e^{-j\pi \sin \psi_{22}} \\ -e^{-j(\pi/2)\alpha_2} & -e^{j(\pi/2)\alpha_1} & -e^{j\pi \sin \psi_{22}} & \sigma^2 + 3 \end{bmatrix} \quad (125)$$

where

$$\begin{aligned} c &= \sigma^2 (4 + \sigma^2) \\ \alpha_1 &= \sin \psi_{12} + \sin \psi_{22} \\ \alpha_2 &= \sin \psi_{12} - \sin \psi_{22} \end{aligned} \quad (126)$$

The SINR of an adaptive array with optimum beamforming is given by [54]:

$$\text{SINR} = \mathbf{U}_d^H \mathbf{R}_{nn}^{-1} \mathbf{U}_d \quad (127)$$

Using (120) and (125) in (127), the SINR for the combined beamforming array after some manipulation becomes:

$$\text{SINR} = -2 \frac{\left(\cos(\pi \sin \psi_{12}) + \cos(\pi \sin \psi_{22}) + 2 \cos(\pi \alpha_1 / 2) - 2\sigma^2 - 6 + 2 \cos(\pi \alpha_2 / 2) \right)}{\sigma^2 (4 + \sigma^2)} \quad (128)$$

4.2.3 Analytical Evaluation of the SINR of Combined Beamforming vs. Independent Beamforming With a Single Interferer

It has been established in section 4.2.1 that the SINR of the individual array output signals combined with optimum combining is equal to the SINR of the individual arrays. The SINR of the individual arrays with independent beamforming has also been derived. In section 4.2.2, the SINR of the arrays for combined beamforming has been derived. In this section it will be shown that the SINR of combined beamforming is greater or equal to the SINR of independent beamforming.

The ratio Γ of the combined beamforming SINR in (128) and the independent beamforming SINR in (112) is:

$$\Gamma = \frac{[\cos(\pi \sin \psi_{12}) + \cos(\pi \sin \psi_{22}) + 2 \cos(\pi \alpha_1 / 2) - 2\sigma^2 - 6 + \cos(\pi \alpha_2 / 2)](\sigma^2 + 2)}{(\sigma^2 + 4)(\cos(\pi \sin \psi_{12}) - 2 - 2\sigma^2 + \cos(\pi \sin \psi_{22}))} \quad (129)$$

where

$$\begin{aligned} \alpha_1 &= \sin \psi_{12} + \sin \psi_{22} \\ \alpha_2 &= \sin \psi_{12} - \sin \psi_{22} \end{aligned} \quad (130)$$

Since $\sigma^2 \ll 1$, equation (129) can be simplified to:

$$\Gamma = \frac{\cos(\pi \sin \psi_{12}) + \cos(\pi \sin \psi_{22}) + 2 \cos(\pi \alpha_1 / 2) - 6 + \cos(\pi \alpha_2 / 2)}{2 (\cos(\pi \sin \psi_{12}) - 2 + \cos(\pi \sin \psi_{22}))} \quad (131)$$

The relation between the angles ψ_{12} and ψ_{22} from the geometry in Figure 30 is:

$$\psi_{22} = \arctan\left(\frac{\sin \psi_{12}}{\xi - \cos \psi_{12}}\right) \quad (132)$$

where ξ is the proportion of the range from array 1 to the mobile relative to the distance between the two arrays. Inserting the angle relationship of (132) into (131), the following is achieved:

$$\Gamma = \frac{4 \cos(\pi \sin \psi_{12} / 2) \cos(\pi \sin \psi_{12} / 2\xi) + \cos(\pi \sin \psi_{12} / \xi) + \cos(\pi \sin \psi_{12}) - 6}{2 (\cos(\pi \sin \psi_{12}) - 2 + \cos(\pi \sin \psi_{12} / \xi))} \quad (133)$$

where

$$\zeta = \sqrt{\xi^2 - 2\xi \cos \psi_{12} + 1} \quad (134)$$

Substituting $\pi \sin \psi_{12} = \omega$ in (133), the following results:

$$\Gamma = \frac{4 \cos(\omega/2) \cos(\omega/2\zeta) + \cos(\omega/\zeta) + \cos(\omega) - 6}{2 (\cos(\omega) - 2 + \cos(\omega/\zeta))} \quad (135)$$

Equation (135) can be simplified further by substituting $\alpha = \frac{\omega}{\zeta}$:

$$\Gamma = \frac{4 \cos(\omega/2) \cos(\alpha/2) + \cos(\alpha) + \cos(\omega) - 6}{2 (\cos(\omega) - 2 + \cos(\alpha))} \quad (136)$$

Using the trigonometric relationship [60]:

$$\cos(a) = \cos^2(a/2) - 1 \quad (137)$$

equation (136) becomes:

$$\Gamma = \frac{4 \cos(\omega/2) \cos(\alpha/2) + \cos^2(\alpha/2) + \cos^2(\omega/2) - 4}{2 (\cos^2(\omega/2) - 2 + \cos(\alpha))} \quad (138)$$

which can be rewritten as:

$$\Gamma = \frac{(\cos(\alpha/2) + \cos(\omega/2))^2 - 4}{2 (\cos^2(\omega/2) + \cos^2(\alpha/2) - 2)} \quad (139)$$

by using the property that [58]

$$(\cos(a) + \cos(b))^2 = \cos^2(a) + 2 \cos(a) \cos(b) + \cos^2(b) \quad (140)$$

Examining equation (139) it can be seen that Γ becomes equal to one in the limit when $\alpha \rightarrow 0$ and $\omega \rightarrow 0$ (which is the case when $\psi_{12} \rightarrow 0$). This indicates that the combined and independent beamforming is equal when the interfering signal comes close in angle to the desired signal. For all other angles, equation (139) is always greater than one, indicating that the SINR of the combined beamforming array is greater than the independent beamforming arrays.

4.2.4 Numerical Evaluation of the SINR of Combined Beamforming vs. Independent Beamforming For Two Interferers

It is difficult to extend the analytical formulation of the ratio of the SINR of the combined beamforming arrays to independent beamforming arrays to more than one interferer. The case for two interferers will be illustrated numerically in this section. The geometry under consideration is shown in Figure 33.

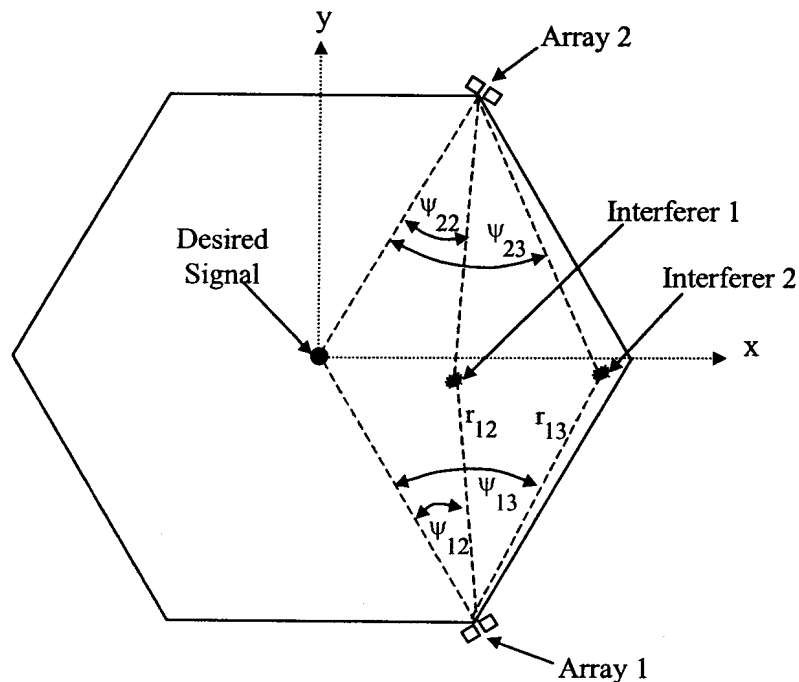


Figure 33: Geometry of two distributed arrays with two interferers.

The SINR is shown in Figure 34 for two fixed angles $\psi_{12} = 20^\circ$ and 40° . In each case the angle ψ_{13} is varied between 0 and 180 degrees. The relationship between the angles is given in (132). The range between array 1 and the two mobiles is equal to 0.4 times the distance between the two arrays, or $\xi = 5/2$ in equation (132). The noise power is 0.001W and the power of the signal and each interferer is equal to 1W.

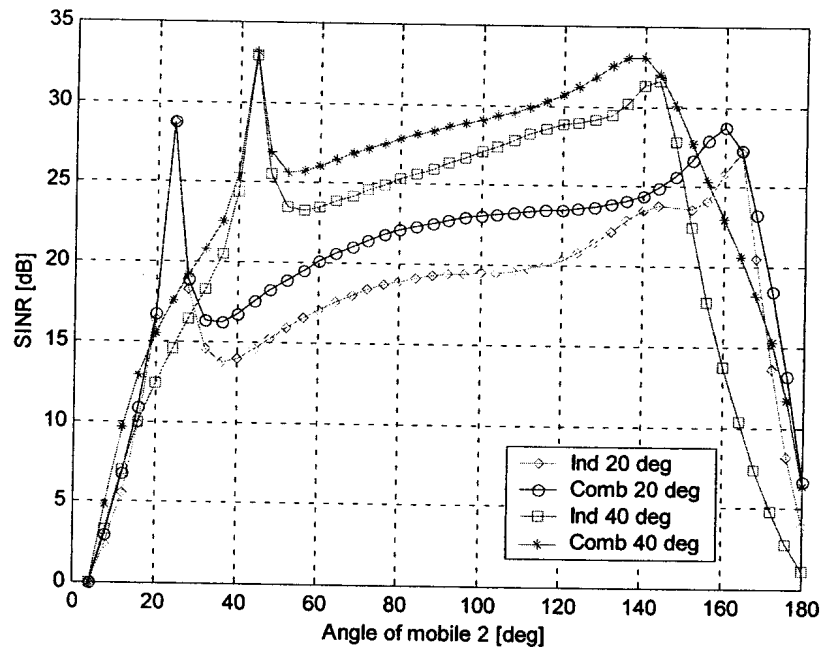


Figure 34: SINR of individual and combined beamforming arrays for ψ_{12} equal to 10° and 20° .

It can be seen in Figure 34 that the SINR of combined beamforming is always greater or equal to the SINR of independent beamforming of the two arrays.

4.2.5 Discussion of the Results of Independent vs. Combined Beamforming

It was shown in the previous sections that the SINR of combined beamforming is always greater or equal to that of independent beamforming for the same number of array elements and for one or two interferers. The fact that the interferer is located on both sides of boresight for the two arrays allowed the combined array to achieve a better cancellation of the interferer. It is an additional “degree of freedom” for the combined array relative to the independent array. It will be shown in later sections that the bit error rate and outage probability of the combined array is significantly better than the arrays combined with independent optimum combining of the arrays.

4.3 Simulated SINR Performance of Distributed Arrays in a Non-Multipath Environment with Three Interferers and Six Elements Per Array

In this section the SINR of distributed arrays will be compared to conventional arrays located at the cell center. In addition the SINR performance of distributed arrays with

combined beamforming of the sub-arrays will be compared to independent sub-array beamforming. The general simulation parameters are as given in Table 2:

Table 2: General simulation parameters

Parameter	Value
Multipath	No
SNR	15 dB
Cell range	1000 m
Reuse factor	3
Number of interferers	3
Signal amplitude (Desired and interferers)	1 (0dB)

The mobile positions are fixed, with the range and angle between the x-axis and the mobiles given in Table 3. The mobiles are all located in the sector covered by array 1 at the cell center, and therefore the SINR of this array only will be compared to the distributed sub-array located at the cell corners.

Table 3: Range and angle of arrival of desired signal and interferers

Array Number	Signal	Range [m]	Angle relative to x-axis [deg]
Center	Desired	500	60
	Interferer 1	500	20
	Interferer 2	500	85
	Interferer 3	100	60
One	Desired	499	240
	Interferer 1	696	267.5
	Interferer 2	586	219
	Interferer 3	900	240
Two	Desired	1322	101
	Interferer 1	1037	92
	Interferer 2	1438	108.5
	Interferer 3	1053	115.3

Array Number	Signal	Range [m]	Angle relative to x-axis [deg]
Three	Desired	1322	19
	Interferer 1	1479	6.6
	Interferer 2	1156	25.5
	Interferer 3	1053	4.72

4.3.1 SINR of Signals In a Single Cell

In this section the SINR performance of conventional center cell arrays and distributed arrays are compared for a single cell with and without power control.

4.3.1.1 SINR Performance Without Power Control

The relative output power as a function of angle for center array one is shown in Figure 35, with six element arrays, three interferers and pathloss exponent of 3.

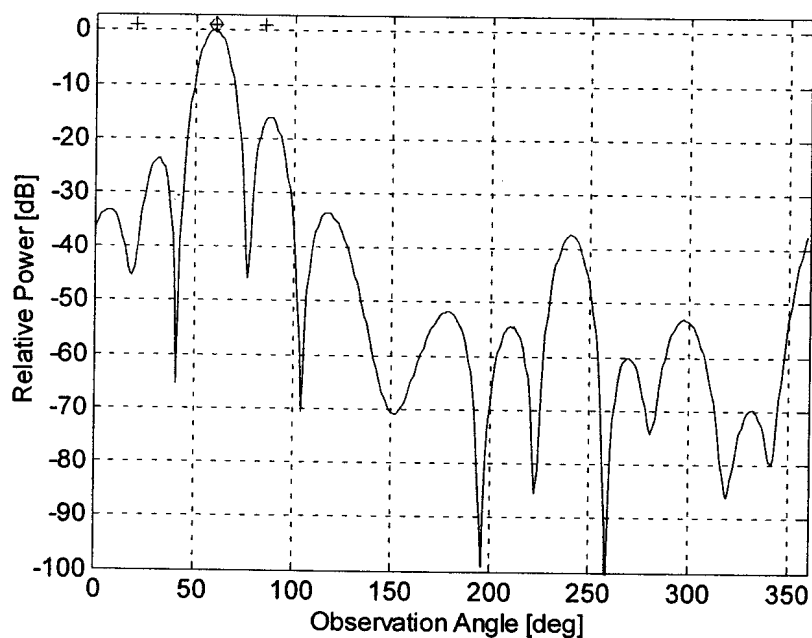


Figure 35: Desired signal received power at center array 1 (Desired Signal indicated with ◊ and interferers with +).

The received signal of the conventional six element arrays at the center of the cell is shown in Figure 36 for pathloss exponent of 3. The figure shows that cancellation of the interferer (interferer 3) in the same direction as the desired signal is difficult to achieve.

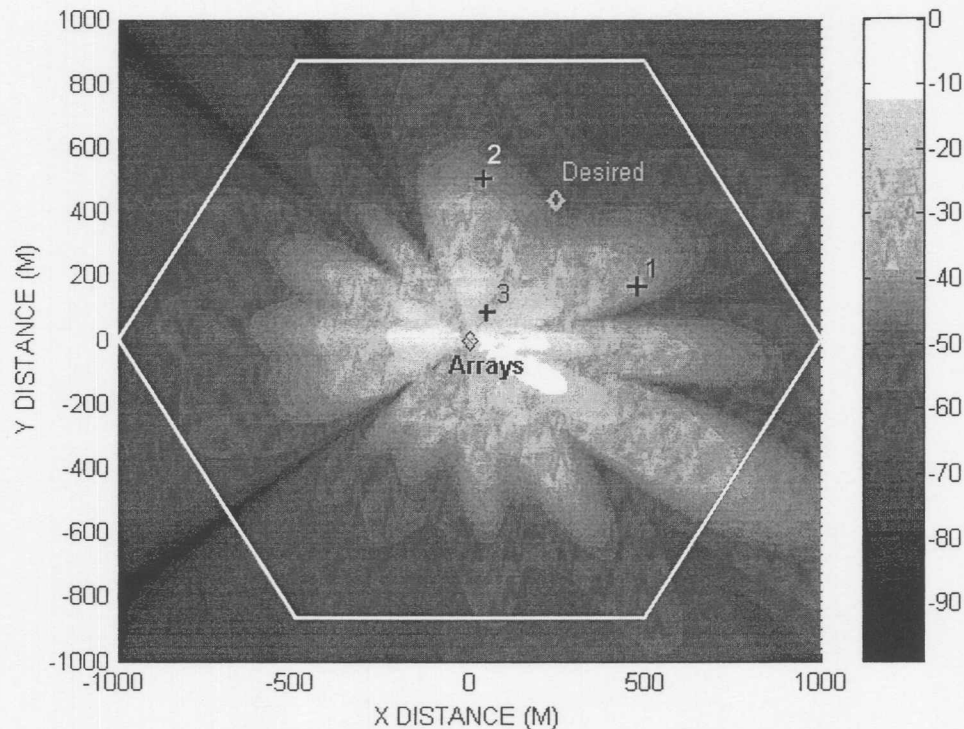


Figure 36: Normalized received power (optimized for the SINR of the desired signal) at the output of the conventional arrays at the cell center in the presence of three interferers (Desired Signal indicated with \diamond and interferers with $+$).

The output power as a function of angle for distributed sub-arrays 1, 2 and 3 with independent beamforming and six element arrays is shown in Figure 37, Figure 38 and Figure 39, respectively. In Figure 37, it can be seen that the signals from interferers 1 and 2 was reduced by more than 40dB. However the signal from interferer 3, which is in the same direction as the desired signal) could not be reduced. On the other hand, since all three interferers are seen from different angles by array 2 (see Figure 38) and array 3 (see Figure 39) and the angles are not overlapping (or close to) with the desired signal incidence angle, these arrays are able to separate the signals.

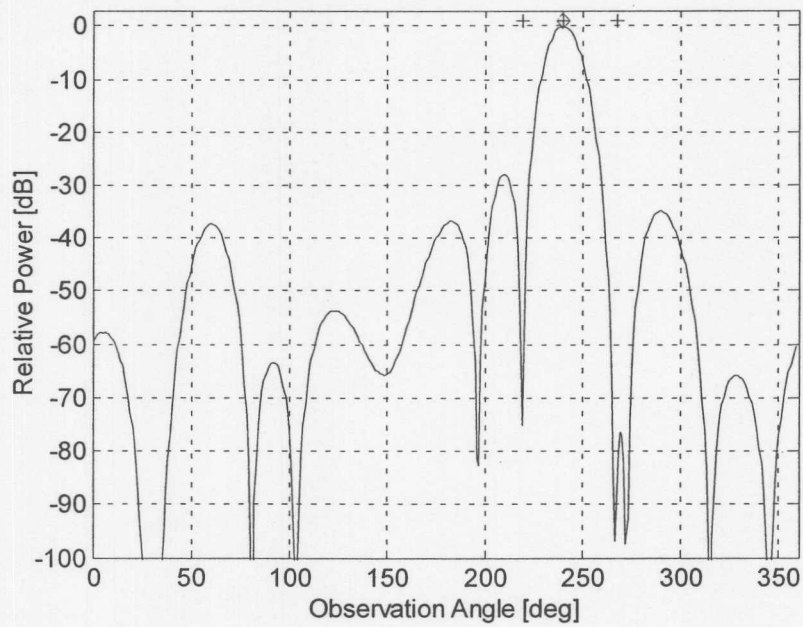


Figure 37: Desired signal received power at array 1 (Desired signal indicated with ◊ and interferers with +).

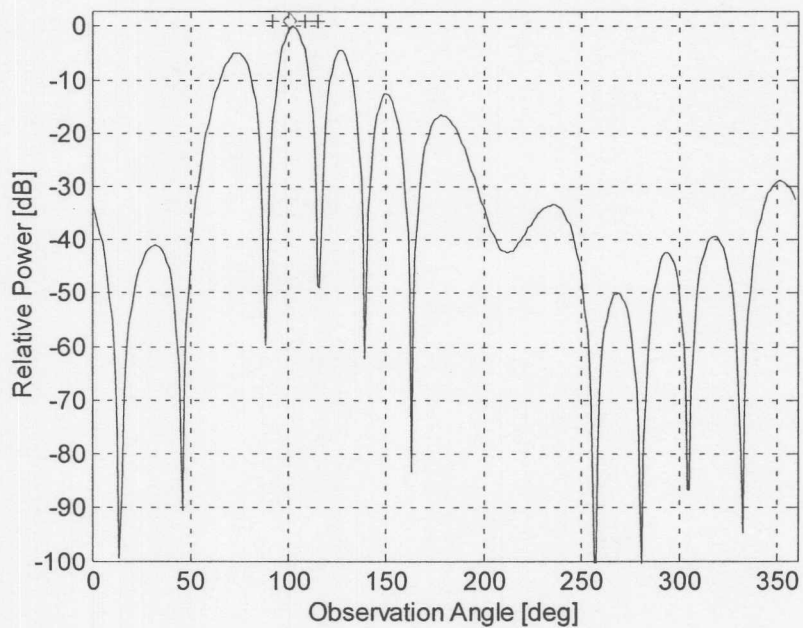


Figure 38: Desired signal received power at array 2 (Desired signal indicated with ◊ and interferers with +).

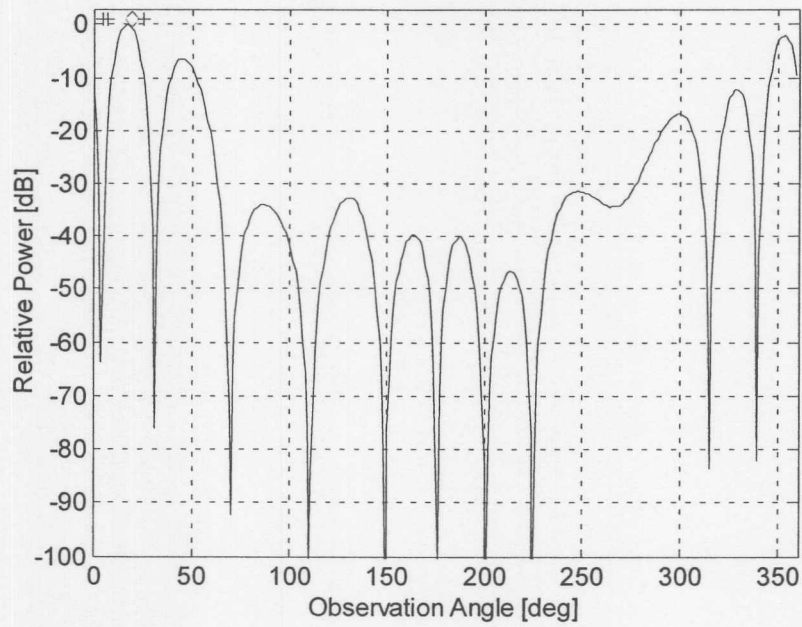


Figure 39: Desired signal received power at array 3 (Desired signal indicated with ◊ and interferers with +).

The received signal at the output of the combined array across the cell area is shown in Figure 40 for six element arrays. It can be seen that the combined array is able to reduce the signals from all three the interferers.

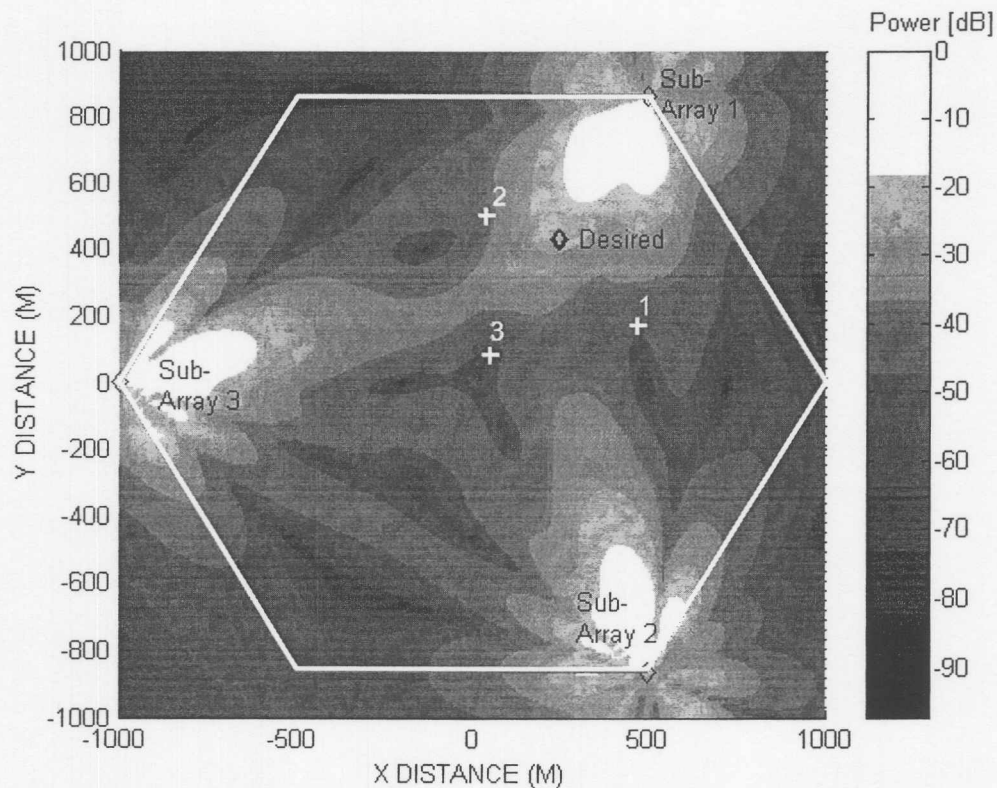


Figure 40: Desired signal normalized received power at the output of the combined distributed array in the presence of three interferers (Desired signal indicated with \diamond and interferers with +).

The SINR of the conventional array at the center of the cell and distributed sub-arrays at the cell corners with independent and combined beamforming is given in Table 4. The independent SINR is the sum of the SINR of all three arrays. The results show that the SINR of the distributed array with combined beamforming is 35dB higher than the conventional center array and 6dB higher than the distributed array with independent beamforming. The SINR of distributed array 1 with independent beamforming is higher than the other two arrays. This is due to the fact that interferer 3 is further in range than that of the desired signal and the other two interferers. The loss to interferers is therefore higher with smaller associated interference than the other two interferers (as seen by sub-array 1).

Table 4: SINR for the distributed array with full sectors, individual arrays and combined array.

Array	SINR [dB]
Distributed full sector	-22.68
Center array	-16.24

Array	SINR [dB]
Array 1	12.02
Array 2	3.68
Array 3	4.03
Independent distributed array beamforming	13.17
Combined distributed array beamforming	19.23

4.3.2 SINR Performance with Power Control

In the following results, power control was applied according to the power control range method described in section 2.5.5.1 for six element arrays with pathloss equal to 3. The power is controlled by the array nearest to the mobile, with the result that a mobile closer to the center of the cell, in case of the distributed array, will transmit the most power. The received power at the center array is shown in Figure 41. Here the angle of arrival of interferer 2 is the same as that of the desired signal. Therefore, the received power from this interferer cannot be reduced by the array. In contrast, the power from the other two interferers has been reduced by more than 30dB.

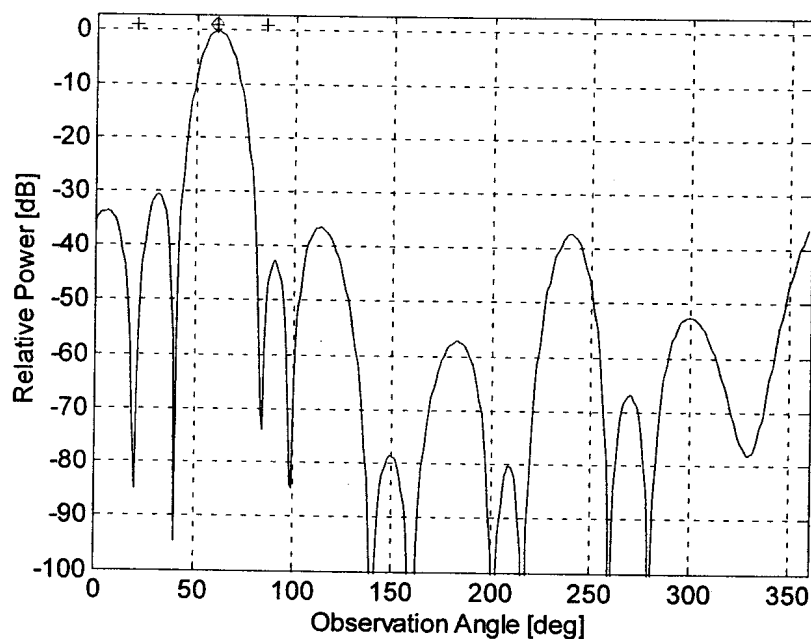


Figure 41: Received power at center array 1 with power control (Desired Signal indicated with ◊ and interferers with +).

The power received by distributed sub-arrays 1,2 and 3 with independent beamforming is given in Figure 42, Figure 43 and Figure 44 respectively. The SINR of the conventional array at the center of the cell and distributed arrays at the cell corners with independent and combined beamforming of the sub-arrays is given in Table 5. The SINR of the combined array is approximately equal for both the power controlled and non-controlled cases. In the case of the center array, the received power of interferer 2 is reduced to be equal to the received power from the other two interferers. The result is that the center array with power control has an improved SINR relative to the non-power controlled case.

Table 5: SINR for the distributed array with full sectors, individual arrays and combined array with power control enabled.

Array	SINR [dB]
Distributed full sector	-7.49
Center array	4.70
Array 1	4.70
Array 2	2.24
Array 3	2.91
Independent distributed array beamforming	8.18
Combined distributed array beamforming	19.15

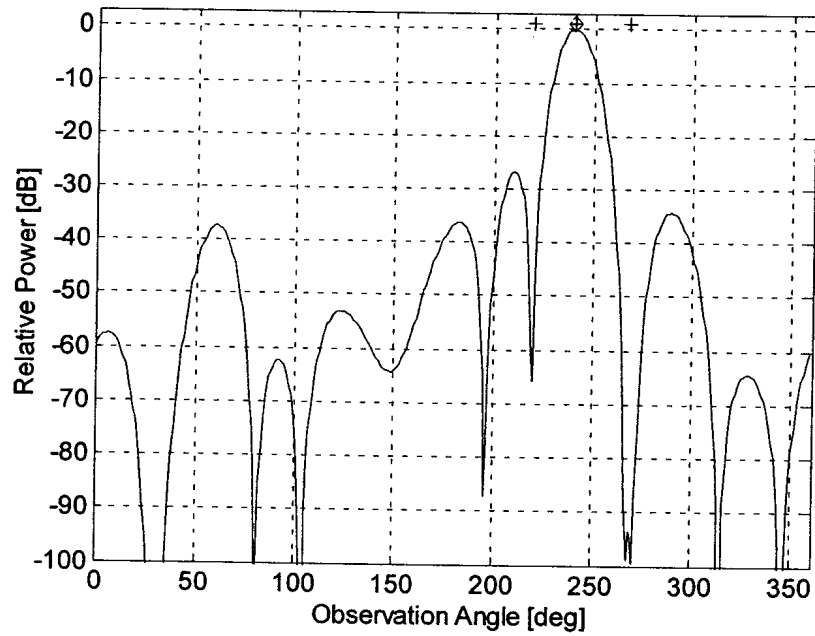


Figure 42: Received power at array 1 with power control enabled (Desired signal indicated with ◊ and interferers with +).

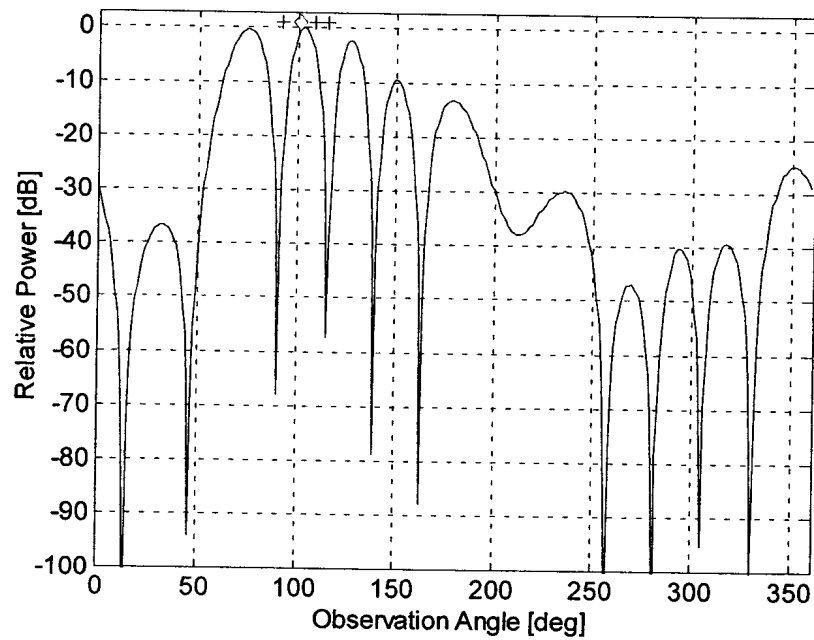


Figure 43: Received power at array 2 with power control enabled (Desired signal indicated with ◊ and interferers with +).

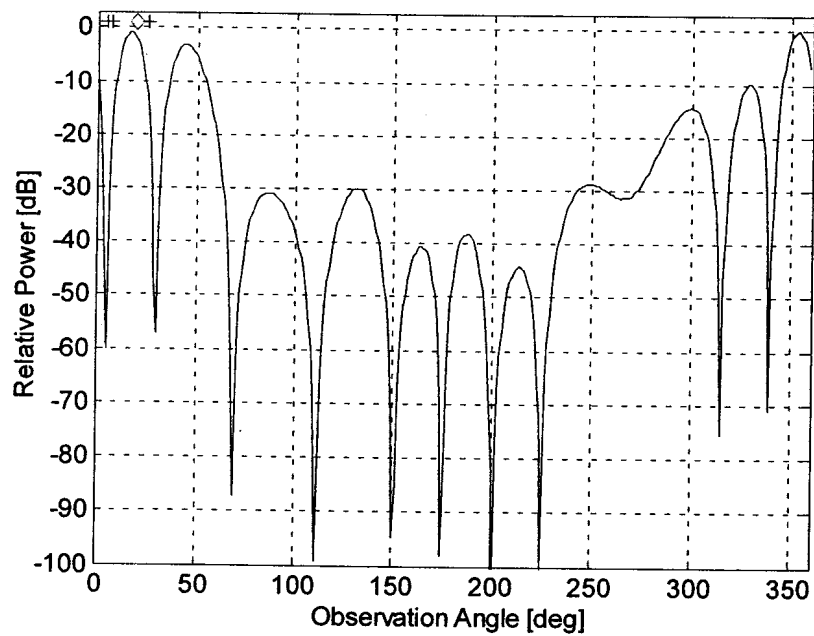


Figure 44: Received power at array 3 with power control enabled (Desired signal indicated with ◊ and interferers with +).

4.3.3 SINR of Signals in a Seven Cell Network (Includes First Tier of Interference)

In this section the SINR performance of conventional center cell arrays and distributed arrays are compared for a seven cell network with and without power control.

4.3.3.1 SINR Performance without Power Control

The received power at the output of distributed six element sub-arrays 1,2 and 3 is shown in Figure 45, Figure 46 and Figure 47 respectively. The pathloss exponent is three.

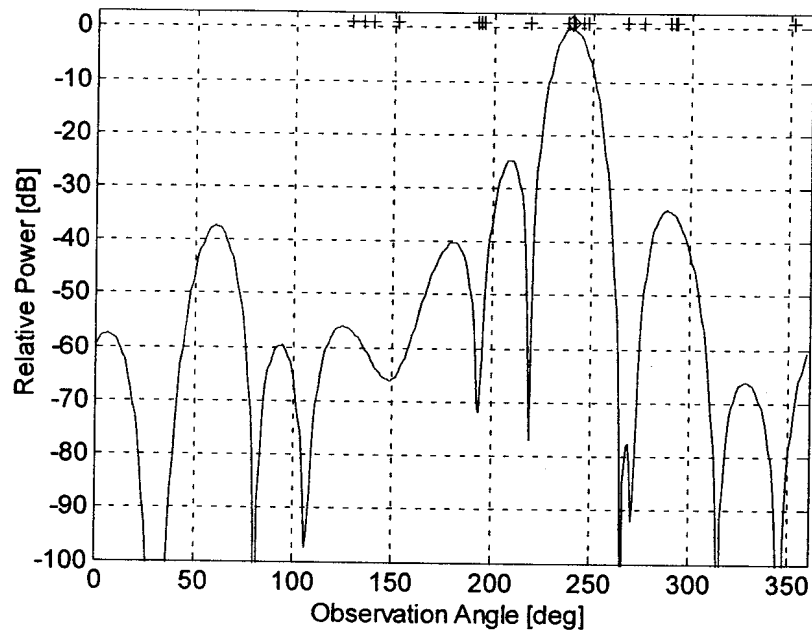


Figure 45: Received power at array 1 without power control in a seven cell configuration (Desired signal indicated with ◊ and interferers with +).

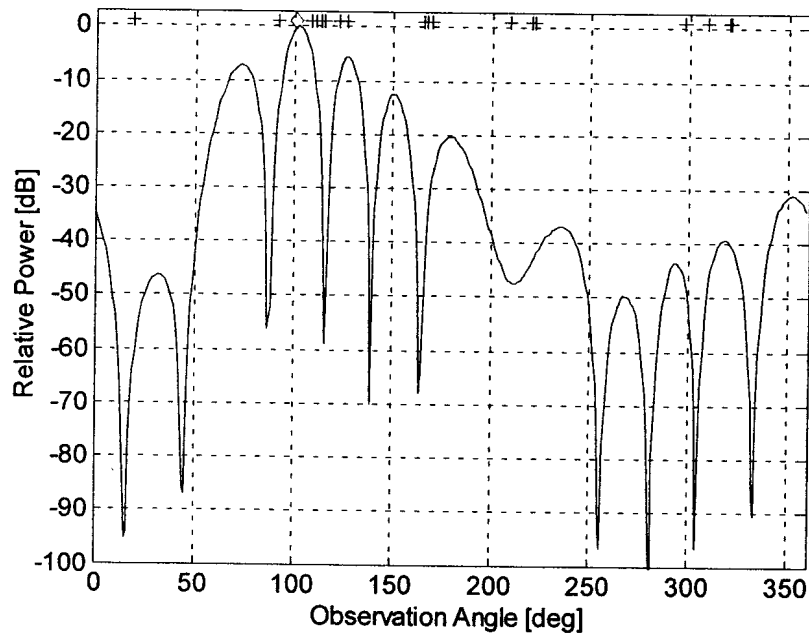


Figure 46: Received power at array 2 without power control in a seven cell configuration (Desired signal indicated with ◊ and interferers with +).

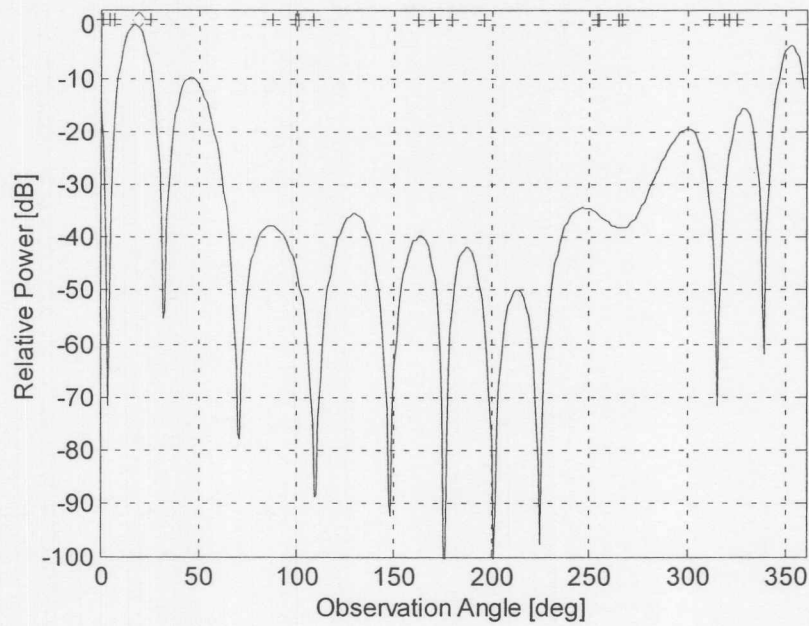


Figure 47: Received power at array 3 without power control in a seven cell configuration (Desired signal indicated with \diamond and interferers with +).

The received power at the output of the combined distributed array is shown in Figure 48 for the seven cell configuration without power control.

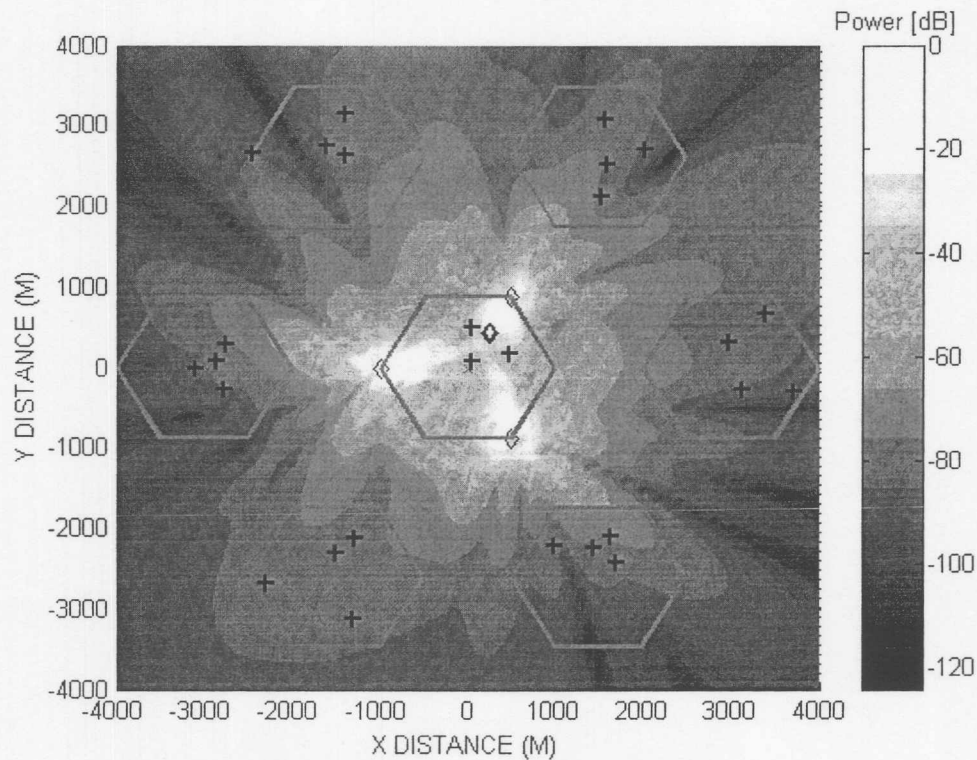


Figure 48: Received signal at combined array without power control in a seven cell configuration (Desired signal indicated with \diamond and interferers with +).

The SINR of the conventional array at the cell center as well as individual and combined beamforming distributed arrays in a seven cell network with power control is given in Table 6. It can be seen that the results are similar to the single cell without power control, but are somewhat lower due to the additional interference from the surrounding cells.

Table 6: SINR without power control of a conventional center cell array and distributed arrays with independent and combined beamforming in a seven cell network.

Array	SINR [dB]
Distributed full sector	-23.66
Center array	-16.19
Array 1	11.91
Array 2	3.23
Array 3	3.59
Independent distributed array beamforming	12.99
Combined distributed array beamforming	18.33

4.3.3.2 SINR Performance with Power Control

The SINR with range power control of the conventional array at the cell center as well as individual and combined beamforming distributed arrays in a seven cell network is given in Table 7. Similar to the SINR of the single cell with and without power control, the SINR of the center in a seven cell network is higher with power control due to the decrease in the power of the interferer close to the base station. The overall SINR of the combined and independent beamforming arrays in a seven cell network with power control is lower than the single cell SINR with power control due to the additional out of cell interference.

Table 7: SINR with power control of the conventional center cell array and distributed arrays with independent and combined beamforming in a seven cell network.

Array	SINR [dB]
Distributed full sector	-8.99
Center array	4.61
Array 1	4.58
Array 2	0.5
Array 3	1.48
Independent distributed array	13.19

Array	SINR [dB]
beamforming	
Combined distributed array beamforming	16.05

4.4 Conclusions

The signal to interference plus noise ratio (SINR) of the distributed array was investigated in this chapter in the absence of multipath components. Closed form expressions for the SINR of two distributed arrays (each with two elements) with independent and combined beamforming were developed. It was shown analytically that the optimum combined SINR of the individual array output signals (after independent beamforming) is equal to the sum of the individual SINRs of the arrays with independent beamforming. Analytical expressions were derived to show that the SINR of two distributed sub-arrays (each with two elements) with combined beamforming is greater or equal to the SINR of independent beamforming of the arrays for a single interferer. It was also shown numerically that this result can be extended to multiple interferers.

The SINR of independent and combined beamforming of distributed arrays in a non-multipath environment was compared by means of simulation results with conventional arrays at the cell center for one desired signal and three same-cell co-channel interferers. Results indicate that for a seven cell network, mobile range power control, six element arrays and pathloss exponent of three the SINR of the combined beamforming array is approximately 11dB higher the SINR of the conventional center array and 3dB higher the SINR of distributed arrays with independent beamforming.